



Enhancing Construction Site Safety: A Risk Modeling Approach

Chengqian Li¹, Manjiang Li^{1,2}, Zhengjun Xia^{1,2}, Xiaoyu Hou^{1*}

¹ School of Civil Engineering, Hunan University, Changsha 410082, China

² Construction Supervision Co., Ltd., Hunan University, Changsha 410082, China

E-mail: cqqli@hnu.edu.cn (Chengqian Li),
2795971984@qq.com (Manjiang Li), 657994111@qq.com (Zhengjun
Xia), 657994111@qq.com (Zhengjun Xia), *HXYhouxy@163.com (Xiaoyu
Hou)

Abstract. Traditional risk assessment methods at construction sites typically rely on manual inspections. These assessments are static and primarily conducted before construction, making it challenging to respond in real-time to the constantly changing environment during construction. This paper proposes a real-time risk assessment and dynamic visualization method for construction sites based on multi-source data fusion, combining data obtained through advanced technologies with data and expertise from traditional methods. By collecting and integrating various data sources such as drone images and fixed surveillance videos, the YOLOv8 model is used for target detection, and depth estimation technology is employed to determine the real-time distance between potential hazards and nearby objects. The method incorporates information from hazard source risk assessment reports generated through manual inspections and utilizes an improved TOPSIS method for dynamic risk assessment of the detected results. Finally, the risk distribution is visually presented through heat maps and other visualization techniques. Experimental results demonstrate that this method can efficiently and accurately identify, assess, and warn of risks during the construction process, providing robust support for safety management at construction sites.

Keywords: Risk Assessment; Risk Visualization; Construction Site Safety; TOPSIS Model

1 Introduction

Construction sites are highly dynamic and complex environments with various potential safety hazards. Traditional risk assessment methods primarily rely on manual inspections, which are static and typically conducted before construction begins. These methods suffer from limited monitoring scope, poor real-time capabilities, and difficulty in accurately identifying and assessing risks, making them inadequate for real-time monitoring and dynamic risk assessment during construction.

As construction progresses, the site environment and risk factors continuously change. Static risk assessment methods fail to provide timely warnings and effective safety management, as they cannot respond in real time to on-site changes or offer ongoing safety assurance throughout the construction process [2, 6]. The advancement of artificial intelligence technology provides an effective means for the real-time detection and notification of hazards on construction sites. [5]. Despite extensive research in this area, there remains a predominant focus on isolated safety risks, such as collisions and hazardous actions, rather than on the comprehensive risk evaluation and decision-making processes vital for robust safety management [3]. Moreover, numerous potential risk factors are often ignored until they become manifestly unsafe behaviors.

To address these challenges, this study introduces an innovative approach for real-time risk assessment and dynamic visualization at construction sites based on multi-source data fusion. By applying advanced analytical techniques, this method aims to provide a more accurate and timely identification of potential hazards, thus enhancing safety management and reducing the occurrence of accidents on construction sites.

2 Methodology Framework

To achieve real-time risk assessment and dynamic visualization at construction sites, this study proposes a comprehensive framework with three main components: risk identification, risk assessment, and risk visualization (Fig. 1).

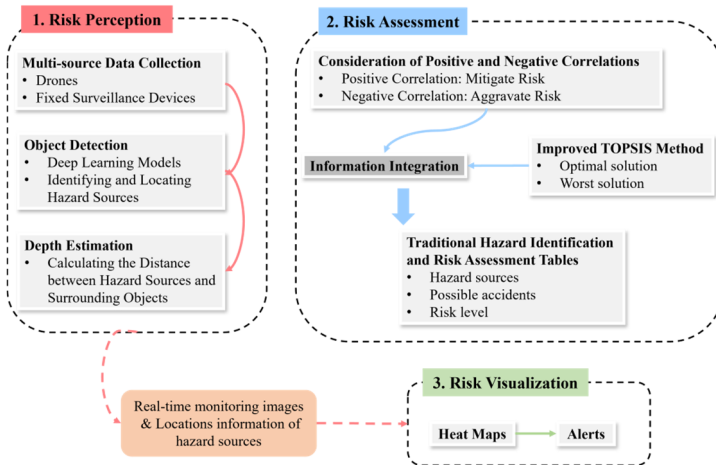


Fig. 1. Real-Time Risk Assessment and Dynamic Visualization Framework

3 Model and Method

In this investigation, the YOLOv8 model is implemented for detecting construction-related objects. After training, the model identifies hazards and related objects by logging bounding box coordinates. For each hazard, positively and negatively associated

objects are marked as $P_{i,j}$ and $N_{i,k}$ respectively. Central coordinates of hazards and nearby objects are recorded. Using MonoDepth2 [4], we estimate pixel depth to convert 2D coordinates into 3D space, adjusting for real-world scaling. Overlapping bounding boxes are considered as having zero distance. This method enhances safety risk monitoring and management on construction sites.

This study gathered hazard identification and risk assessment checklists from over 40 construction projects. These checklists, typically issued before construction begins, detail common accident causes and their potential safety impacts. By leveraging computer vision technology, the study identified high-risk hazard sources from these checklists and calculated their potential accident risk levels using a specific formula:

$$r_i = \sum_{z=1}^{IV} (e_{i,z} * q_{e_{i,z}}) / \sum q_{e_{i,z}} \tag{1}$$

Construction site safety regulations require a critical "safety distance" to reduce hazards (Fig. 2). Two important distance thresholds have been identified by experts to understand spatial interactions between risk factors:

Critical Distance (a): Interaction intensity between risk factors remains stable within this threshold and can be seen as constant.

Critical Distance (b): Interaction intensity decreases between distances "a" and "b". Beyond distance "b", changes in interaction intensity become negligible and can be ignored.

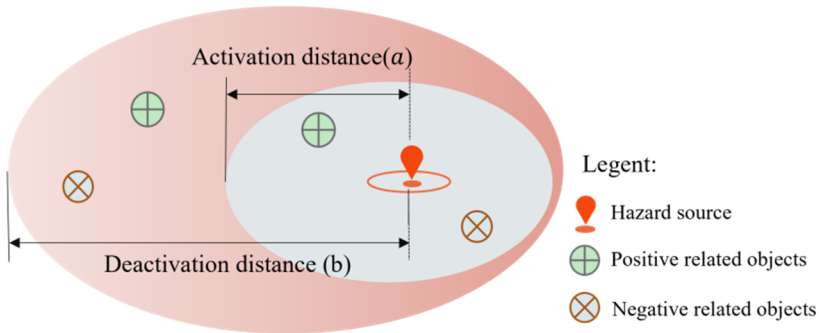


Fig. 2. Optimal and Worst Influence Distances for Hazard Impact at Construction Sites

Assessing risk is challenging due to hazards interacting over space and time. The TOPSIS method offers a solution by comparing real scenarios with the best and worst possible cases. [1].

In practical engineering, multiple objects may be positively or negatively correlated with varying numbers and distances. To address this complexity, the TOPSIS method calculates the spatial coupling risk impact factor β based on the proximity of these objects. The influence coefficients β_p and β_n of risk-related factors, encompassing objects with both positive and negative correlations, are calculated using Eq. (2).

$$\beta_{p/n} = \frac{d_{p/n}^-}{d_{p/n}^+ + d_{p/n}^-} \tag{2}$$

The total risk score for the hazard is computed using Equation (3):

$$R_i = \frac{r_i}{2} (1 - \beta_p + \beta_n) \quad (3)$$

Fig. 3 shows some examples of how the effects of different combinations of associated objects vary with distance.

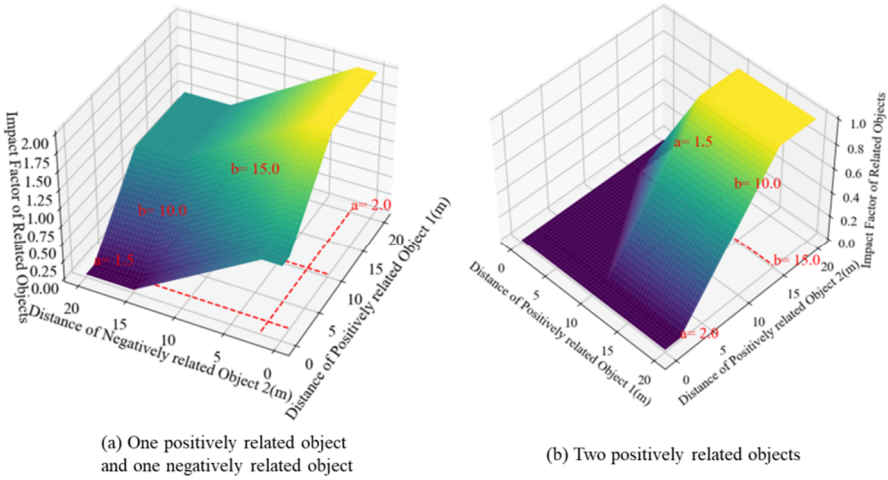


Fig. 3. Impact Utility Variation with Distance for Related Objects.

Risk visualization diagrams are valuable tools for illustrating the outcomes of risk assessments and conveying potential hazards to workers. These diagrams, created by computers, visually represent risks on construction sites to aid in risk reduction. They employ colors to denote different risk levels, taking into account comprehensive risk values near hazard sources. The process involves: (1) Storing the hazard source's center of mass and risk value in a three-dimensional array. (2) Creating a coordinate matrix, computing distances between data and grid points, and using a Gaussian function to determine weight values. (3) Generating an elevation map and assigning colors based on weight values. (4) Aligning the map with the original 2D image and refining colors and parameters.

4 Experiments and Results

This study collected data from two main sources: drone aerial photography and fixed monitoring videos. Drones captured 28,240 images across various construction sites in Changsha, China, featuring 38 different object types. Additionally, 60 video segments, each 180 seconds long, documented major construction phases over a week. Traditional risk assessment reports were also incorporated, providing detailed hazard information.

After extracting key frames from the video data of the experimental scene, target recognition and depth estimation were performed. The results are shown in the middle

part of Fig. 4. The hazard source in both images is identified as the same excavator. Detection also revealed that the negatively correlated object, a car, changes its distance from the moving excavator over time. Specifically, when the distance between the car and the excavator is 5.12 m at time t_1 , the average comprehensive risk value of the excavator is 59. When the distance decreases to 3.61 m at time t_2 , the average comprehensive risk value increases to 67. These risk values at different times are used to generate a heat map, displayed in Fig. 4.

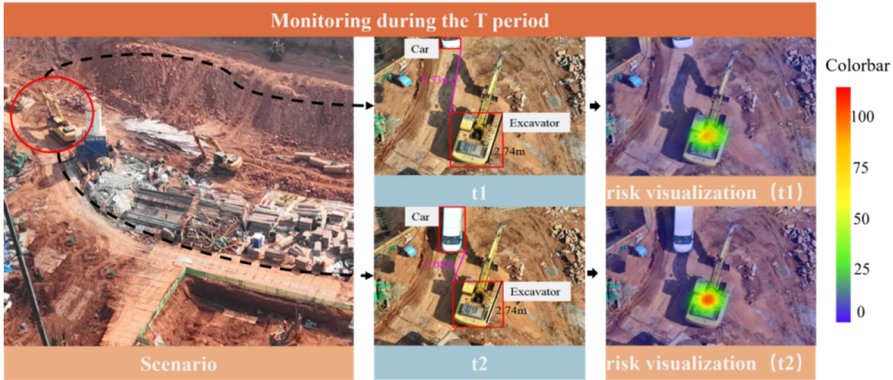


Fig. 4. Risk heat map for scenario

5 Conclusion

Since traditional safety risk identification methods cannot achieve real-time risk management during construction, this study proposes a real-time risk assessment and dynamic visualization method for construction sites based on multi-source data fusion, combining data obtained from advanced technologies with those from traditional methods and experiences. This study achieves the automation of quantifying and visualizing safety risks in construction by integrating computer vision techniques with quantitative risk assessment methods. It focuses on monitoring potential risk factors, evaluating risks through real-time monitoring of changes in the quantity and distance of hazard sources, thereby enhancing traditional risk identification and prediction methods. Experimental results demonstrate a high consistency rate of 95% between the proposed model and expert assessments. Future research aims to optimize the model further, improve its robustness in complex environments, and explore additional application scenarios.

Despite the effectiveness of our approach, it has limitations primarily due to inherent challenges in computer vision, such as occlusion, difficulty in identifying small objects, and insufficient lighting during nighttime or adverse weather conditions. Future research will aim to address these issues by integrating additional data sources, enhancing image processing algorithms, and employing advanced AI techniques to improve robustness and accuracy in diverse and challenging environments.

Acknowledgement

This research received support from (1) the National Natural Science Foundation of China (Grant No. 72201095, 72101275), (2) Foundation items: National Key Research and Development Program of China (No.2023YFC3806800), and (3) Hunan Provincial Natural Science Foundation (Grant No. 2023JJ40189, 2022JJ40645).

References

1. Behzadian, M., Otaghsara, S. K., Yazdani, M., and Ignatius, J., "A state-of-the-art survey of TOPSIS applications," *Expert Systems with Applications*, vol. 39, no. 17, pp. 13051-13069, 2012, doi: <https://doi.org/10.1016/j.eswa.2012.05.056>.
2. Chen, H., Luo, X., Zheng, Z., and Ke, J., "A proactive workers' safety risk evaluation framework based on position and posture data fusion," *Automation in Construction*, vol. 98, pp. 275-288, 2019, doi: <https://doi.org/10.1016/j.autcon.2018.11.026>.
3. Fang, W., Zhong, B., Zhao, N., Love, P. E., Luo, H., Xue, J., and Xu, S., "A deep learning-based approach for mitigating falls from height with computer vision: Convolutional neural network," *Advanced Engineering Informatics*, vol. 39, pp. 170-177, 2019, doi: <https://doi.org/10.1016/j.aei.2018.12.005>.
4. Godard, C., Mac Aodha, O., Firman, M., and Brostow, G. J., "Digging into self-supervised monocular depth estimation," presented at the The IEEE/CVF International Conference on Computer Vision, 2019.
5. Xiao, B., Lin, Q., and Chen, Y., "A vision-based method for automatic tracking of construction machines at nighttime based on deep learning illumination enhancement," *Automation in Construction*, vol. 127, p. 103721, 2021, doi: <https://doi.org/10.1016/j.autcon.2021.103721>.
6. Zhang, S., Boukamp, F., and Teizer, J., "Ontology-based semantic modeling of construction safety knowledge: Towards automated safety planning for job hazard analysis (JHA)," *Automation in Construction*, vol. 52, pp. 29-41, 2015, doi: <https://doi.org/10.1016/j.autcon.2015.02.005>.

Open Access This chapter is licensed under the terms of the Creative Commons Attribution-NonCommercial 4.0 International License (<http://creativecommons.org/licenses/by-nc/4.0/>), which permits any noncommercial use, sharing, adaptation, distribution and reproduction in any medium or format, as long as you give appropriate credit to the original author(s) and the source, provide a link to the Creative Commons license and indicate if changes were made.

The images or other third party material in this chapter are included in the chapter's Creative Commons license, unless indicated otherwise in a credit line to the material. If material is not included in the chapter's Creative Commons license and your intended use is not permitted by statutory regulation or exceeds the permitted use, you will need to obtain permission directly from the copyright holder.

